Differential encoding of fear learning and fear expression in the ventral and dorsal hippocampus

Marco N. Pompili[1,2,*,§], Noé Hamou[1,2,*], & Sidney I. Wiener[1]

While there is substantial evidence that the dorsal and ventral hippocampus play different roles during emotional learning, it is unknown how these roles are implemented. Here, we simultaneously recorded multiple single units in these structures during fear conditioning, and demonstrated a predominance of responses related to fear expression in dorsal hippocampus, while ventral hippocampal responses were more closely linked with the acquisition of conditioned fear. Furthermore, cell assemblies containing both dorsal and ventral synchronously active neurons emerged during fear conditioning, suggesting a potential substrate to integrate these complementary signals for learning and behavior.

INTRODUCTION

The hippocampus (HPC) has long been recognized as a crucial hub for memory processes and spatial cognition[1]. While the same basic circuitry is maintained throughout the entire structure, there are anatomical, genetic and functional variations along its septo-temporal axis[2,3]. Lesions and pharmacological manipulations in the dorsal (dHPC) and ventral (vHPC) HPC in rodents (respectively, septal and temporal in primates) tend to have distinct effects on spatial vs. emotional learning[4–7]. In fear conditioning paradigms, manipulations of the dHPC impair the formation, consolidation, and retrieval of contextual but not cued fear memory[4,8,9] while vHPC manipulations seem to have broader effects[7,10–13]. This has led to the conventional view that the dHPC primarily processes spatial and contextual information, while the vHPC is more involved in emotional processing[2,3,14].

This dichotomy is supported by neuronal recordings in rodents. First, the precision of spatial coding diminishes along the dorsoventral axis of the HPC[15–18]. Second, neurons in more ventral parts of the HPC exhibit a stronger association with the emotional valence of locations[19–22] and odors[23] as compared to the dHPC. Moreover, recent work further suggests that specific pathways between the vHPC, the amygdala, and the prefrontal cortex are key for anxiety and fear-related behaviors[13,20,24–28].

However, this dominant view is challenged by several results highlighting the involvement of the dorsal hippocampus (dHPC) in emotional processing, beyond its traditional role in contextual or spatial processing. Indeed, under several experimental conditions, suppressing activity in the dHPC impairs trace fear conditioning[29,30]. Additionally, more recent work showed that modulation of fear-related dHPC engram cells impacts both fear expression and anxiety-related behaviors, as observed with manipulation of vHPC engram cells[31–33]. These results support a more nuanced view where both the vHPC and dHPC could contribute to emotional processing, and in particular to fear conditioning. Overall, while an extensive literature supports the notion that dorsal and ventral HPC play different roles in fear learning, their respective contributions remain to be defined.

To study this, we directly compared the neural activity of dHPC and vHPC neurons during Pavlovian fear conditioning. While neural population activity in both dHPC and vHPC varied with fear conditioning, surprisingly, only dHPC neurons were strongly modulated by fear expression, demonstrating that the encoding of emotionally relevant information is not restricted to the ventral hippocampus. On the other hand, vHPC neurons developed specific responses associated with fear learning. Thus, representations related to different aspects of an emotional experience are distributed differentially along the dorsoventral axis of the HPC. Furthermore, during conditioning, we observed the formation of synchronous co-activation of neurons, cell assemblies, composed of both dHPC and vHPC neurons. The emergence of these assemblies provides a potential mechanism through which distinct representations of fear learning and fear expression can be combined to construct an integrated representation of the emotional experience across the whole hippocampus.

RESULTS

To study the neural mechanisms underlying the distinct and shared contributions of dorsal and ventral HPC to fear learning, we simultaneously recorded in these structures in four male rats undergoing classical Pavlovian conditioning. Multiple bundles of twisted microwires were chronically implanted bilaterally in both regions (**Figure 1A** and **Supp. Fig. 1**), enabling the detection of single units (**Fig. 1B**, **Supp. Fig. 2**). The behavioral protocol included two days of habituation sessions (HAB) and two days of fear conditioning (FC; **Fig. 1C**). In order to study the initial acquisition of FC, we analyzed recordings from the first day of conditioning, taking the last day of HAB as a control. During FC, the animals demonstrated freezing responses starting from the second coupling of the conditioned stimulus (CS, pips of pure tones) with the unconditioned stimulus (US, a mild electrical footshock), indicating that the CS-US association was acquired then (**Fig. 1D**).

[1]Centre Interdisciplinaire de Recherche en Biologie (CIRB) - CNRS UMR 7241 - INSERM U1050, Collège de France, Université PSL, 11 place Marcelin Berthelot, 75005 Paris, France
[2]Current address: Institut de Neurosciences des Systèmes (INS), INSERM UMR1106, Aix-Marseille Université, 27 Boulevard Jean Moulin, 13005 Marseille, France
[*]These authors contributed equally to this work
[§]Correspondence should be addressed to MNP (marco.pompili@normalesup.org)

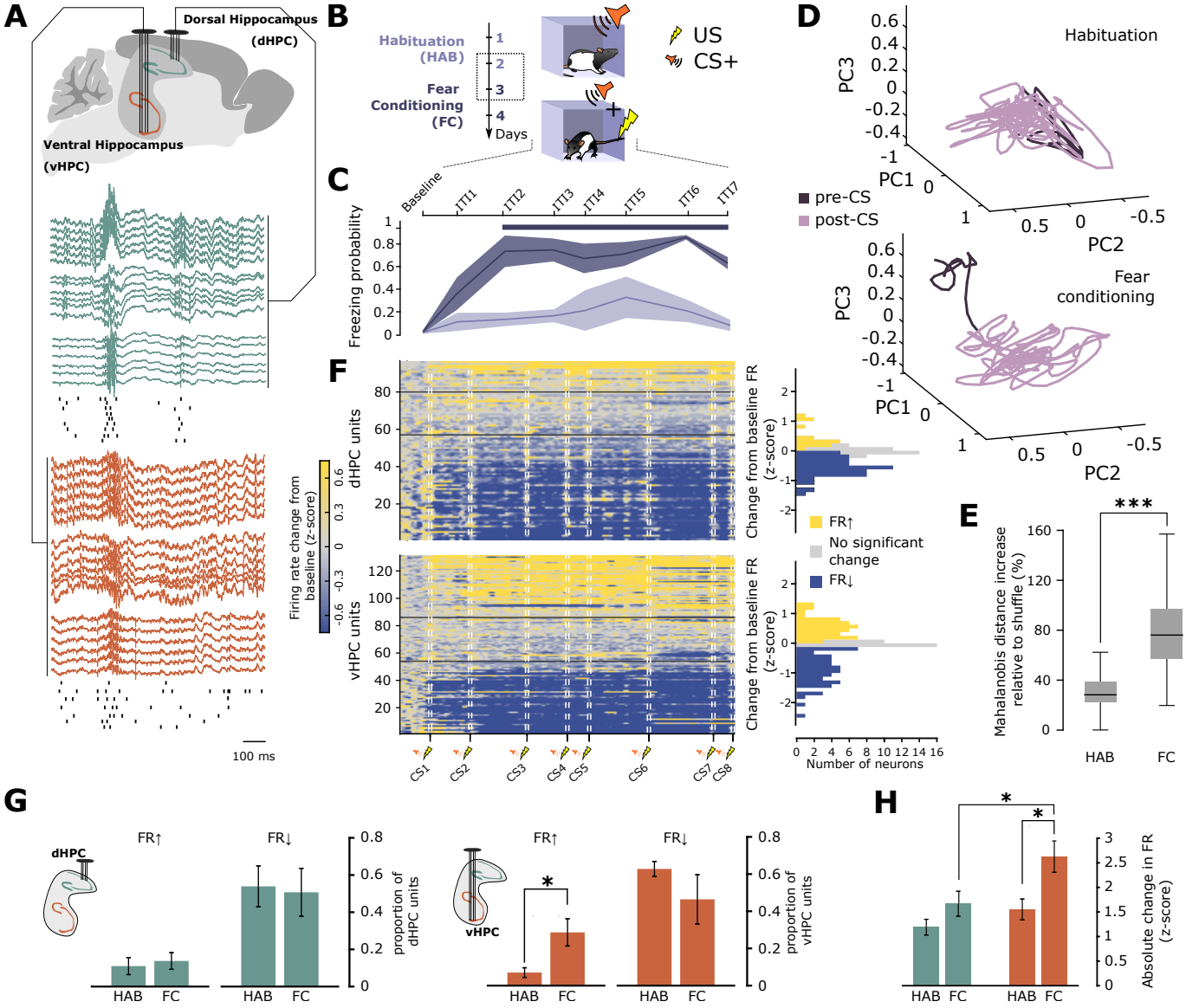

Figure 1. Simultaneous recordings in dorsal and ventral hippocampus reveal population coding shifts and neuronal firing rate changes during fear conditioning.
(**A**) Simultaneous bilateral recordings of single units in dHPC and vHPC (top). Example recordings during awake immobility in both dHPC and vHPC. Raw traces appear above. Sharp wave-ripple events are accompanied by synchronous neuronal activity (below). (**B**) Behavioral protocol. On days 1 and 2, rats underwent habituation (HAB) sessions with auditory tone cues (CS+) but no footshocks. On days 3 and 4, the rats were fear conditioned in the BOX where tone presentations were coupled with foot shocks. (**C**) During the first fear conditioning session, the CS-US association was learned quickly. From CS2 on, the horizontal bar indicates that the freezing probability was significantly higher in the FC session than HAB session ($p < 0.05$, paired t-test). ITI : intertrial interval (the period between successive 20-sec CS presentations). (**D**) Evolution of PCA-projected population spiking activity over time. The first three PCA components are shown for one example animal. The dark purple curve corresponds to the first 3 minutes of recording before presentation of CS1 while lilac corresponds to the period after CS1. (**E**) Comparison between FC and HAB of average spatial shift (Mahalanobis distance) in PCA space between pre- and post-CS1 activity relative to time-shuffled projections for all animals. ($p < 0.001$, Wilcoxon rank-sum test). (**F**) Color plot of normalized firing rate (z-scored and subtracted from baseline) during the FC session. Baseline: period before CS1. Horizontal black bars (left) separate neurons with significantly ($p < 0.05$) increasing (FR↑) and decreasing firing rates (FR↓). Histograms (right) show the distribution of their firing rate changes. (**G**) Comparison of relative proportions in neuronal responses. (H) Magnitude of change in firing rate (z-scored).

Shifts in hippocampal population activity during fear conditioning

We initially investigated whether there were any changes in neuronal population activity during fear acquisition. For this, principal component analysis (PCA) reduced the high-dimensional multi-neuronal activity of each recording onto lower-dimensional spaces. This showed that global HPC population activity shifts significantly more after the first CS during FC than in HAB (**Fig. 1D-E**). This global shift in the PCA space could reflect changes in neuronal firing rates[34]. Indeed, during FC, neurons significantly changed their firing rate after the first CS (**Fig. 1G**), with increases or decreases in firing rate (**Fig. 1 F,H** and **Supp. Fig. 3**). The majority of HPC neurons tended to decrease their firing rate across both HAB and FC, in concert with the decrease in motor activity observed in both session types (**Supp. Fig. 4**). Indeed, as we observed previously[35], this motor activity decrease is associated either to increases in freezing or rest during FC and HAB, respectively (**Supp. Fig. 4**). These PCA and firing rate shifts are consistent

with previous reports showing FC-associated firing rate changes in the HPC[21,36]. Interestingly, in the vHPC, both the proportion of firing rate-increasing neurons (**Fig 1G**) and the overall firing rate magnitude change (**Fig 1H**) were higher during FC than in HAB. In addition, during FC, the overall magnitude of firing rate change was greater for vHPC than for dHPC neurons (**Fig 1H**). This provides evidence for stronger fear-related rate coding changes in the vHPC than in the dHPC.

Distinct encoding of fear expression in dHPC and fear learning vHPC

To better understand what may drive these differences, we then further examined the responses of dHPC and vHPC neurons to behavioral and task-related events. Neuronal responses to freezing (fear expression) and CSs (fear conditioning) were assessed by computing the firing rate change following the onset of the events (see Methods). Our first hypothesis was that the greater firing rate changes in vHPC were associated with behavioral changes related to fear and freezing increases, since these emerged at and after fear acquisition (**Fig. 1C**). For this, we investigated neuronal

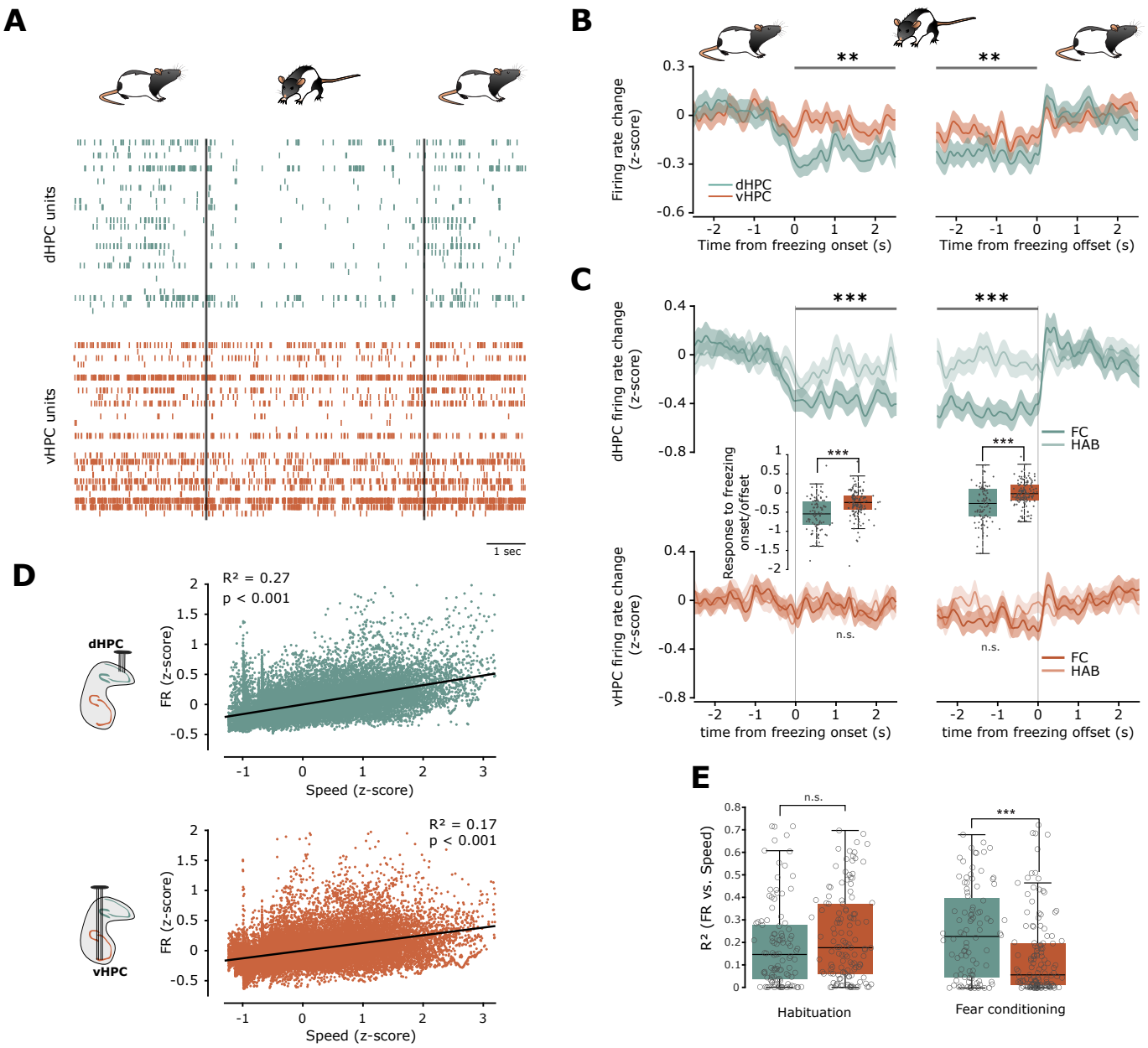

Figure 2. Encoding of fear expression in dHPC

(**A**) Raster plot of dHPC (blue, top) and vHPC (orange, bottom) neurons before, during and after a representative freezing episode (bracketed by vertical bars). (**B**) Average (+/- SEM) firing rate changes in the dHPC and vHPC (see Methods) at freezing onset (left) and offset (right). Bars above curves mark periods when dHPC and vHPC firing rates were significantly different ($p < 0.01$, Wilcoxon rank-sum test). Same color code as in A. (**C**) Comparison of average firing rate changes during FC (dark curves) and during HAB (light curves) at freezing onset (left) and offset (right). Insets compare the corresponding average responses (see Methods) during fear conditioning. No significant difference was detected between HAB and FC for vHPC firing rate (p $<$ 0.001, Wilcoxon ranksum test). (**D**) Linear regression between firing rate and animal's speed. All neurons and all data from FC and HAB sessions (1 s time bins). (**E**) Comparison of the correlation strength (coefficient of determination) of individual neurons for linear regressions of firing rate with speed in dHPC vs. vHPC during HAB and FC ($p < 0.001$, Wilcoxon signed rank test; n.s., not significant).

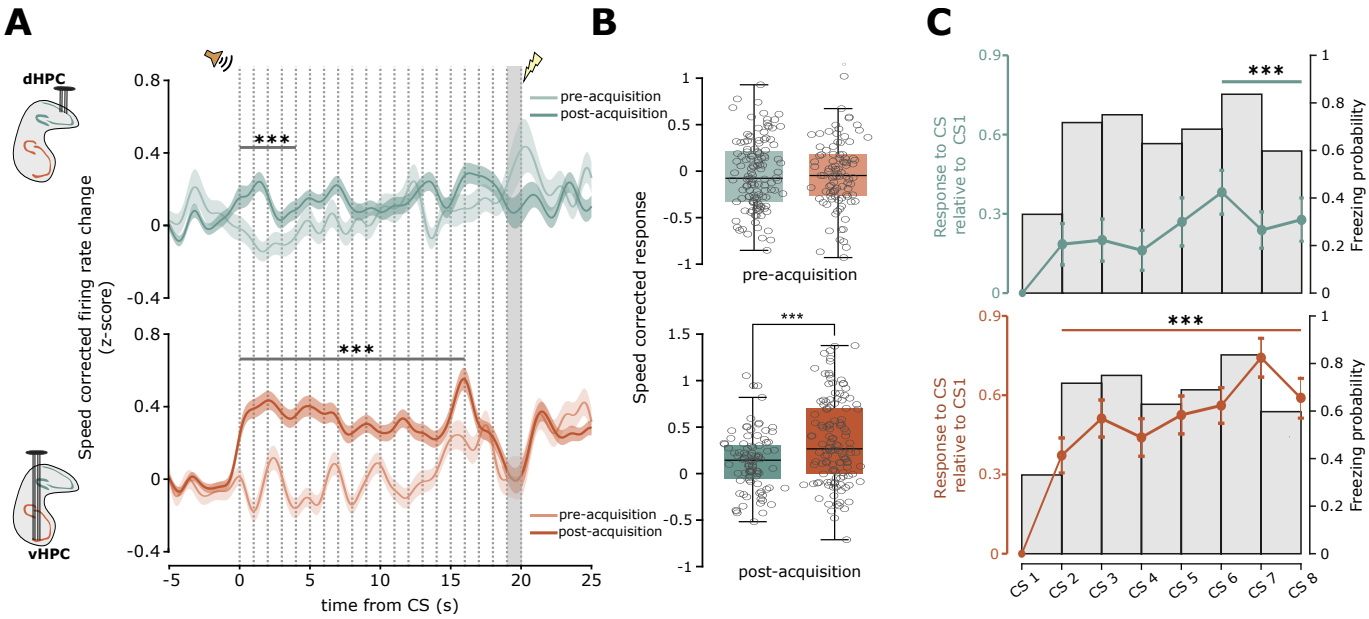

Figure 3. Encoding of fear learning in the vHPC
(**A**) Comparison of neurons' speed-corrected responses to CS before fear acquisition (CS1 and CS2, light curves) and after (CS3 to CS8, dark curves) during the first FC session ($p < 0.001$, Wilcoxon signed rank test). Dotted vertical bars represent individual tone pips within a CS presentation, and the gray shaded bars are the US presentations. (**B**) Comparison of the average responses to CS presentations (during the first 10 seconds after the CS) pre-acquisition (top) and post-acquisition (bottom). Each dot corresponds to the average for one neuron ($p < 0.001$, Wilcoxon rank-sum test). (**C**) CS response change relative to CS1 as baseline (see Methods) compared with freezing probability increase. Horizontal bars above curves show when the CS responses were significantly different from the response to CS1 ($p < 0.001$, Wilcoxon signed rank test).

responses to freezing behavior. On average, dHPC neurons were inhibited during freezing events while vHPC neurons were not (**Figure 2A-B**). This result failed to support our initial hypothesis, and was surprising given the ample published evidence for a role of vHPC in controlling anxiety and fear behavior[13,20,22,24,37]. A possible explanation for the dHPC freezing-associated inhibition would be related to the motor, rather than the emotional, aspects of freezing. Previous work had shown that activity in dHPC is modulated more by animals' speed than vHPC[18]. However, immobility-related inhibition was stronger in dHPC during FC (freezing) compared to immobility periods during HAB (which were not associated with fearful stimuli or mild shocks; **Figure 2C**). Thus, dHPC neurons did not respond exclusively to freezing per se. This was further indicated by the fact that while the firing rate was correlated with animals' motor activity in both dHPC and vHPC (**Figure 2D**), this correlation was significantly greater in dHPC than vHPC during fear conditioning, but not during habituation (**Figure 2E**). Overall, these results suggest that dHPC neurons responded specifically to fearful freezing and, more generally, to movement in a fearful context.

Next, we investigated neuronal responses to CS presentations in order to detect changes associated with emotional learning. After fear acquisition (i.e, after CS2; **Fig. 1B**), neurons in both dHPC and vHPC developed excitatory responses to the CS (**Supp. Fig. 5**). To estimate the response components unrelated to movement, firing rate was corrected based on the linear correlation between firing rate and animal's movement (**Fig. Supp. 6**, see Methods). After this correction, only vHPC neurons retained a robust, sustained responses to the CS after fear acquisition (**Figure 3A-B**). Imporantly, the emergence of these neural responses coincided with acquisition of the tone-shock association (**Figure 3C**). Thus, vHPC neurons become responsive to the contingency between the CS and US, independent of associated behavior. This supports the notion that vHPC plays a role in representing the learned relationship between conditioned stimuli and associated emotional outcomes.

Figure 4. Recruitment of mixed dorsal-ventral assemblies during fear conditioning [figure on following page]
(**A**) Example dHPC-only (top), mixed (middle) and vHPC-only (bottom) assemblies. Each circle corresponds to one neuron. Large colored circles correspond to assembly members and small gray circles to non-members. The length of the bars depict each neuron's contribution (principal component weight) to the assembly. Horizontal dashed lines represent the threshold for a cell to be considered a member of the assembly (see Methods). (**B**) Activity of the dHPC-only (top), mixed (middle), and vHPC-only (bottom) assemblies during FC and HAB sessions. Same color code as D. Vertical bars correspond to CSs occurences. (**C**) Absolute assemblies' activity change after CS1 relative to baseline. (**D**) Average proportions of dHPC-only, vHPC-only and mixed assemblies. Bracket indicates significant difference between proportions ($p < 0.01$, paired t-test). All except mixed HAB are significntly greater than zero ($p < 0.01$) (**E**) Activation strength (top), raster plot of single unit activity (middle), and animal's speed (bottom) during a freezing episode (bracketed by vertical bars at left) and during CS+ presentations in FC1 after acquisition (tone pip onsets and offsets are bracketed by pairs of vertical bars at right). vHPC unit spikes are in red and dHPC in blue. The rows with the gray shading correspond to the assembly members. (**F**) Comparison of the average responses to freezing and conditioning (see Methods) for members of dHPC-only, mixed, and vHPC-only assemblies. Same data points of Figure 2C and 2F but grouped according to assembly composition.

Figure 4. [continued from previous page] Recruitment of mixed dorsal-ventral assemblies during fear conditioning
(**G**) Comparison of the responses to freezing and conditioning (see Methods) of the member neurons grouped by assembly types'. Dots: responses of each assembly member. X's: cluster centers of mass. Shaded areas, contour lines of Gaussian model density estimates of the clusters' distributions. (**H**) Comparison of the distances increases between the clusters in the plots in G relative to clusters with shuffled neuron identities. (**I**) Schematic representation of dHPC-only assembly neurons responding to freezing, vHPC-only assembly neurons to conditioning and mixed assembly neurons to freezing and conditioning.

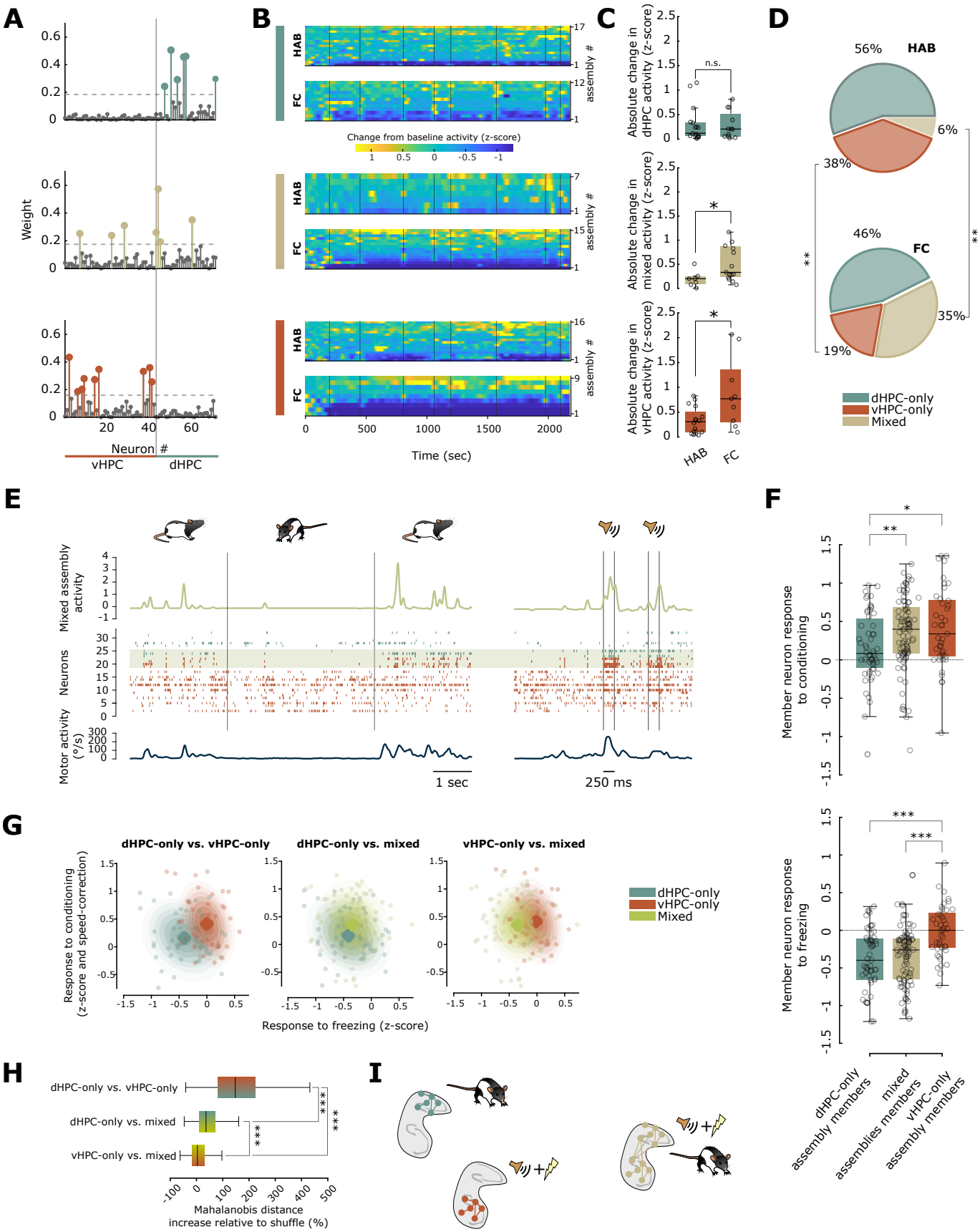

Mutual contribution of dHPC and vHPC to mixed cell assemblies emerging during FC

Finally, we tested whether the neuronal activity in the dHPC and vHPC is coordinated to integrate these representations of fear expression and fear learning. For this, we examined the synchronization across the HPC dorso-ventral axis in each recording session by extracting cell assemblies from PCA components (**Fig. 1E-G**) using ICA[38–40] and studying *mixed assemblies*[39], composed of neurons from both the vHPC and the dHPC (**Figure 4A** and **Supp. Fig. 7**). vHPC-only and mixed assemblies activity rates changed significantly after the first tone-shock association, while dHPC assemblies did not appear to respond to fear acquisition (**Figure 4B-C**). Moreover, while mixed assemblies had a low incidence during HAB, their proportion was significantly higher during FC. In contrast, the proportion of vHPC-only assemblies decreased (**Figure 4D**). This would be consistent with vHPC assemblies recruiting dHPC neurons during FC to form mixed assemblies, possibly integrating signals from both areas. Consistently, while dHPC-only assembly neurons primarily responded to freezing, and vHPC-only assembly neurons to conditioning, neurons in mixed assemblies responded to both freezing and conditioning (**Fig. 3E-H**). This points to a role of mixed assemblies in the integration of hippocampal activity during fear learning and fear expression (**Fig. 3I**).

DISCUSSION

Functional differences between dHPC and vHPC in fear learning have been posited for more than three decades. However, to date, it was still unknown if and how neurons across the HPC dorsoventral axis may differentially encode fearful stimuli and behavior. Here, to our knowledge, we show for the first time, encoding differences between dHPC and vHPC during fear learning.

In summary, the activity profiles of populations of neurons in the hippocampus underwent significant shifts during fear conditioning. These shifts are associated with dHPC neurons predominantly inhibited during freezing, while vHPC neurons increased firing rate concurrently with the acquisition of the CS-US association. Neurons with these distinct responses are recruited during fear conditioning by mixed dorsal-ventral assemblies. This provides a potential mechanism for integrating responses of individual cells within multifactorial hippocampal-wide engrams representing both learning and its associated behavioral response. To our knowledge, this is the first report of simultaneous recording of behavioral correlates of single units in dorsal and ventral HPC. It must be noted that some vHPC-only and dHPC-only assemblies might be part of larger mixed assemblies that were not detected.

Crucially, while past studies only compared neural activity before vs. after conditioning[21,36], here we were able to record neural activity during FC. This enabled to directly study how neural activity is modulated by learning, and to show that HPC representations rapidly adapt their coding schemes after a single presentation of the CS-US association. This suggests a potential mechanisms underpinning the acquisition of conditional fear memory after a single CS-US pairing[41].

Anatomical connectivity gradients could explain the different responses observed in the vHPC and dHPC. The vHPC has stronger bilateral connections with the amygdala[13,20,24,28] than the dHPC, and the amygdala is the first structure to encode the CS-US association during FC[42]. Consistently, we observed the acquisition of excitatory responses to the CS in the vHPC, and an increase in the proportion of firing rate increasing cells in the vHPC during fear conditioning. Anatomical gradients in the HPC might therefore underlie 'representational gradients', along which different features of experience are processed. As suggested in a recent study, dHPC and vHPC circuits could then broadcast information about these different features to distinct downstream brain structures to support memory[43].

The acquisition of a freezing-specific response in dHPC neurons challenges the notion that the dHPC is restricted to spatial and contextual processing, but is consistent with a recent report showing that optogenetic stimulation of dHPC, but not vHPC during FC increases freezing[44]. These results extend a new perspective: the dHPC could encode a more comprehensive representation of the animal's state relative to its environment. This expanded representation would not only include spatial but also emotional states, such as fearful freezing states. Conversely, the vHPC may predominantly represent external environmental contingencies, such as the CS-US association. To be able to respond to an imminent threat, the brain needs to rapidly bind these distinct representations together. Here, these complementary representations emerge rapidly during fear conditioning, after only one or two CS-US presentations, and are combined in mixed assemblies. Our study thus provides insights into the respective representations emerging in the dHPC and vHPC during fear conditioning and underscores their collective role in orchestrating an adaptive response.

ACKNOWLEDGMENTS We thank Gabriel Makdah and Eulalie Leroux for help with data acquisition and Ralitsa Todorova for useful discussions. This work was funded by a Labex MemoLife grant to SIW and MNP.

AUTHOR CONTRIBUTIONS Research project design: MNP, SIW, NH. Experiments: MNP. Data analysis design: MNP, NH, SIW. Data analysis: NH. Writing and results visualisation: MNP, NH, SIW

COMPETING INTERESTS The authors declare no competing interests.

REFERENCES

[1] G. Buzsáki and E. I. Moser. "Memory, navigation and theta rhythm in the hippocampal-entorhinal system". In: *Nature Neuroscience* 16.2 (2013), pp. 130–138.

[2] M. S. Fanselow and H.-W. Dong. "Are the Dorsal and Ventral Hippocampus Functionally Distinct Structures?" In: *Neuron* 65.1 (2010), pp. 7–19.

[3] B. A. Strange, M. P. Witter, E. S. Lein, and E. I. Moser. "Functional organization of the hippocampal longitudinal axis". In: *Nature Reviews Neuroscience* 15.10 (2014), pp. 655–669.

[4] J. J. Kim and M. S. Fanselow. "Modality-Specific Retrograde Amnesia of Fear". In: *Science* 18 (1992).

[5] E. Moser, M.-B. B. Moser, and P. Andersen. "Spatial learning impairment parallels the magnitude of dorsal hippocampal lesions, but is hardly present following ventral lesions". In: *Journal of Neuroscience* 13.9 (1993), pp. 3916–3925.

[6] D. M. Bannerman, M. A. Good, B. K. Yee, M. J. Heupel, S. D. Iversen, and J. N. Rawlins. "Double dissociation of function within the hippocampus: A comparison of dorsal, ventral, and complete hippocampal cytotoxic lesions". In: *Behavioral Neuroscience* 113.6 (1999), pp. 1170–1188.

[7] S. Maren and W. G. Holt. "Hippocampus and Pavlovian Fear Conditioning in Rats : Muscimol Infusions Into the Ventral , but Not Dorsal , Hippocampus Impair the Acquisition of Conditional Freezing to an Auditory Conditional Stimulus". In: *Behavioral Neuroscience* 118.1 (2004), pp. 97–110.

[8] R. G. Phillips and J. E. LeDoux. "Differential Contribution of Amygdala and Hippocampus to Cued and Contextual Fear Conditioning". In: *Behavioral Neuroscience* 106.2 (1992), pp. 274–285.

[9] I. Goshen, M. Brodsky, R. Prakash, J. Wallace, V. Gradinaru, C. Ramakrishnan, and K. Deisseroth. "Dynamics of retrieval strategies for remote memories." In: *Cell* 147.3 (2011), pp. 678–689.

[10] J. L. Rogers, M. R. Hunsaker, and R. P. Kesner. "Effects of ventral and dorsal CA1 subregional lesions on trace fear conditioning". In: *Neurobiology of Learning and Memory* 86.1 (2006), pp. 72–81.

[11] M. R. Hunsaker and R. P. Kesner. "Dissociations across the dorsal-ventral axis of CA3 and CA1 for encoding and retrieval of contextual and auditory-cued fear". In: *Neurobiology of Learning and Memory* 89.1 (2008), pp. 61–69.

[12] M. E. Wang, N. P. Fraize, L. Yin, R. K. Yuan, D. Petsagourakis, E. G. Wann, I. a. Muzzio, and W. E. T. Al. "Differential roles of the dorsal and ventral hippocampus in predator odor contextual fear conditioning". In: *Hippocampus* 23 (2013), pp. 451–466.

[13] C. Xu et al. "Distinct Hippocampal Pathways Mediate Dissociable Roles of Context in Memory Retrieval". In: *Cell* 167.4 (2016), 961–972.e16.

[14] É. Pronier, J. F. Morici, and G. Girardeau. "The role of the hippocampus in the consolidation of emotional memories during sleep". In: *Trends in Neurosciences* 46.11 (2023), pp. 912–925.

[15] B. Poucet, C. Thinus-Blanc, and R. U. Muller. "Place cells in the ventral hippocampus of rats." In: *Neuroreport* 5 (1994), pp. 2045–2048.

[16] M. W. Jung, S. I. Wiener, and B. L. McNaughton. "Comparison of spatial firing characteristics of units in dorsal and ventral hippocampus of the rat". In: *The Journal of Neuroscience* 14.December (1994), pp. 7347–7356.

[17] K. B. Kjelstrup, T. Solstad, V. H. Brun, T. Hafting, S. Leutgeb, M. P. Witter, E. I. Moser, and M.-B. Moser. "Finite scale of spatial representation in the hippocampus." In: *Science (New York, N.Y.)* 321.5885 (2008), pp. 140–3.

[18] J. R. Hinman, S. C. Penley, L. L. Long, M. A. Escabí, and J. J. Chrobak. "Septotemporal variation in dynamics of theta: Speed and habituation". In: *Journal of Neurophysiology* 105.6 (2011), pp. 2675–2686.

[19] S. Ciocchi, J. Passecker, H. Malagon-Vina, N. Mikus, T. Klausberger, H. Malagon-Vina, N. Mikus, and T. Klausberger. "Selective information routing by ventral hippocampal CA1 projection neurons". In: *Science* 348.6234 (2015), pp. 560–563.

[20] N. Padilla-Coreano, S. S. Bolkan, G. M. Pierce, D. R. Blackman, W. D. Hardin, A. L. Garcia-Garcia, T. J. Spellman, and J. A. Gordon. "Direct Ventral Hippocampal-Prefrontal Input Is Required for Anxiety-Related Neural Activity and Behavior". In: *Neuron* 89.4 (2016), pp. 857–866.

[21] S. W. Jin and I. Lee. "Differential encoding of place value between the dorsal and intermediate hippocampus". In: *Current Biology* 31.14 (2021), 3053–3072.e5.

[22] H. Malagon-Vina, S. Ciocchi, and T. Klausberger. "Firing patterns of ventral hippocampal neurons predict the exploration of anxiogenic locations". In: *eLife* 12 (2023), pp. 1–24.

[23] J. S. Biane et al. "Neural dynamics underlying associative learning in the dorsal and ventral hippocampus". In: *Nature Neuroscience* 26.5 (2023), pp. 798–809.

[24] A. C. Felix-Ortiz, A. Beyeler, C. Seo, C. A. Leppla, C. P. Wildes, and K. M. Tye. "BLA to vHPC inputs modulate anxiety-related behaviors." In: *Neuron* 79.4 (2013), pp. 658–64.

[25] H. C. Meyer et al. "Ventral hippocampus interacts with prelimbic cortex during inhibition of threat response via learned safety in both mice and humans". In: *Proceedings of the National Academy of Sciences of the United States of America* 116.52 (2019), pp. 26970–26979.

[26] W. B. Kim and J. H. Cho. "Encoding of contextual fear memory in hippocampal–amygdala circuit". In: *Nature Communications* 11.1 (2020), pp. 1–22.

[27] J. Graham, A. F. D'Ambra, S. J. Jung, Y. Teratani-Ota, N. Vishwakarma, R. Venkatesh, A. Parigi, E. G. Antzoulatos, D. Fioravante, and B. J. Wiltgen. "High-Frequency Stimulation of Ventral CA1 Neurons Reduces Amygdala Activity and Inhibits Fear". In: *Frontiers in Behavioral Neuroscience* 15.March (2021), pp. 1–13.

[28] R. Nguyen, K. Koukoutselos, T. Forro, and S. Ciocchi. "Fear extinction relies on ventral hippocampal safety codes shaped by the amygdala". In: *Science Advances* 9.22 (2023), pp. 1–16.

[29] I. Misane, P. Tovote, M. Meyer, J. Spiess, S. O. O. Ogren, and O. Stiedl. "Time-dependent involvement of the dorsal hippocampus in trace fear conditioning in mice.pdf". In: *Hippocampus* 15 (2005), pp. 418–426.

[30] J. J. Quinn, H. M. Wied, Q. D. Ma, M. R. Tinsley, and M. S. Fanselow. "Dorsal hippocampus involvement in delay fear conditioning depends upon the strength of the tone-footshock association". In: *Hippocampus* 18.7 (2008), pp. 640–654.

[31] X. Liu, S. Ramirez, P. T. Pang, C. B. Puryear, A. Govindarajan, K. Deisseroth, and S. Tonegawa. "Optogenetic stimulation of a hippocampal engram activates fear memory recall." In: *Nature* 484.7394 (2012), pp. 381–385.

[32] B. K. Chen et al. "Artificially Enhancing and Suppressing Hippocampus-Mediated Memories". In: *Current Biology* 29.11 (2019), 1885–1894.e4.

[33] N. T. M. Robinson, L. A. L. Descamps, L. E. Russell, M. O. Buchholz, B. A. Bicknell, G. K. Antonov, J. Y. N. Lau, R. Nutbrown, C. Schmidt-Hieber, and M. Häusser. "Targeted activation of hippocampal place cells drives memory-guided spatial behavior". In: *Cell* 183.6 (2020), pp. 1586–1599.

[34] A. Peyrache, K. Benchenane, M. Khamassi, S. I. Wiener, and F. P. Battaglia. "Principal component analysis of ensemble recordings reveals cell assemblies at high temporal resolution". In: *Journal of computational neuroscience* 29.1-2 (2010), pp. 309–325.

[35] M. N. Pompili and R. Todorova. "Discriminating Sleep From Freezing With Cortical Spindle Oscillations". In: *Frontiers in neural circuits* (2022), p. 15.

[36] M. A. P. Moita, S. Rosis, Y. Zhou, J. E. LeDoux, and H. T. Blair. "Putting fear in its place: remapping of hippocampal place cells during fear conditioning." In: *The Journal of neuroscience : the official journal of the Society for Neuroscience* 24.31 (2004), pp. 7015–7023.

[37] J. C. Jimenez et al. "Anxiety Cells in a Hippocampal-Hypothalamic Circuit". In: *Neuron* 97.3 (2018), 670–683.e6.

[38] V. Lopes-dos-Santos, S. Ribeiro, and A. B. L. Tort. "Detecting cell assemblies in large neuronal populations". In: *Journal of Neuroscience Methods* 220.2 (2013), pp. 149–166.

[39] V. J. Oberto, C. J. Boucly, H. Y. Gao, R. Todorova, M. B. Zugaro, and S. I. Wiener. "Distributed cell assemblies spanning prefrontal cortex and striatum". In: *Current Biology* 32 (2022), pp. 1–13.

[40] M. N. Pompili, C. J. Boucly, R. Todorova, E. M. Leroux, S. I. Wiener, and M. Zugaro. "Flexible communication between cell assemblies and 'reader' neurons". In: *bioRxiv* (2022), p. 2022.09.06.506754.

[41] M. S. Fanselow. "Factors governing one-trial contextual conditioning". In: *Animal Learning & Behavior* 18.3 (1990), pp. 264–270.

[42] G. J. Quirk, J. C. Repa, and J. E. LeDoux. "Fear conditioning enhances short-latency auditory responses of lateral amygdala neurons: Parallel recordings in the freely behaving rat". In: *Neuron* 15.5 (1995), pp. 1029–1039.

[43] M. Sosa, H. R. Joo, and L. M. Frank. "Dorsal and Ventral Hippocampal Sharp-Wave Ripples Activate Distinct Nucleus Accumbens Networks". In: *Neuron* 105.4 (2020), 725–741.e8.

[44] F. Fredes, M. A. Silva, P. Koppensteiner, K. Kobayashi, M. Joesch, and R. Shigemoto. "Ventro-dorsal Hippocampal Pathway Gates Novelty-Induced Contextual Memory Formation". In: *Current Biology* 31.1 (2021), 25–38.e5.

[45] L. Hazan, M. Zugaro, and G. Buzsáki. "Klusters, NeuroScope, NDManager: a free software suite for neurophysiological data processing and visualization". In: *Journal of neuroscience methods* 155.2 (2006), pp. 207–216.

[46] M. O. Pasquet et al. "Wireless inertial measurement of head kinematics in freely-moving rats". In: *Scientific Reports* 6.October (2016), pp. 1–18.

[47] G. Paxinos and C. Watson. *The Rat Brain in Stereotaxic Coordinates - 7th edition.* Academic Press, 2013, p. 472.

[48] G. Makdah, S. I. Wiener, and M. N. Pompili. "Detection of Cell Assemblies in High-Density Extracellular Electrophysiological Recordings". In: *bioRxiv* (2024).

METHODS

Animals Four male Long-Evans rats (350–400 g at the time of surgery) were housed individually in monitored conditions (21°C and 45% humidity) and maintained on a 12h light – 12h dark cycle. In order to avoid obesity, food was restricted to 13–16 g of rat chow per day, while water was available ad libitum. To habituate the rats to human manipulation, they were handled each workday. All experiments conformed to the approved protocols and regulations of the local ethics committee (Comité d'éthique en matière d'expérimentation animale Paris Centre et Sud n°59), the French Ministries of Agriculture, and Research.

Surgery The rats were deeply anesthetized with ketamine-xylazine (Imalgene 180 mg/kg and Rompun 10 mg/kg) and anesthesia was maintained with isoflurane (0.1-1.5% in oxygen). Analgesia was provided by subcutaneous injection of buprenorphine (Buprecaire, 0.025 mg/kg) and meloxicam (Metacam, 3 mg/kg). The animals were implanted with a custom-built prosthesis with 42 independently movable hexatrodes (bundles of 6 twisted tungsten wires, 12 μm in diameter, gold-plated to $\sim$200 kΩ). The electrode tips were implanted 0.5 mm above the CA1 pyramidal layer of dHPC and vHPC -5 to -4.5 mm posterior and +/- 3.8 to 5 mm lateral from bregma. Miniature stainless steel screws were implanted above the cerebellum to serve as electrical reference and ground. During recovery from surgery (minimum 7 days), the rats received antibiotic (Marbofloxacine, 2 mg/kg) and analgesic (Meloxicam, 3 mg/kg) treatments via subcutaneous injections and were provided with food and water ad libitum. The recording electrodes were then progressively lowered until sharp wave ripple and single unit activity was visible and adjusted to optimize yield and stability of single-units.

Behavioral apparatus Two environmental contexts (BOX and CYL) were used for the fear conditioning protocol. The BOX context was a cubicle conditioning chamber (40x40x40 cm) with gray PVC walls lined with ribbed black rubber sheets and a floor composed of nineteen stainless steel rods (0.48 cm diameter with 1.6 cm intervals) connected to a scrambled shock generator (ENV-414S, Med Associates, USA). It was scented daily with mint cleaning solution (Simple Green, Sunshine Makers). The CYL context was a stadium-shaped enclosure (30 cm straight sides and 15 cm radius) with a black wooden floor, and walls lined with light brown pieces of rope rug. It was scented daily with a vanilla extract solution. A custom-made system presented the animals with two auditory CSs (80 dB, 20 s long, each composed of 250 ms long pips of either white noise as CS+, or an 8 kHz pure tone as CS-, presented once per second). During each session, after a baseline period of 3 min, the animals were presented to 16 CS (8 CS+ and 8 CS-), separated by intervals ranging between 120 and 200 s. Only CS+ presentations were analyzed.

Behavioral protocol Each experimental day, rats were placed in both contexts for 35 min to ensure that any behavioral differences observed between the two environments were not related to their familiarity. Before and after recording sessions, animals were allowed to rest in a cloth-lined plastic flowerpot (30 cm upper diameter, 20 cm lower diameter, 25 cm high). On days 1 and 2, rats underwent habituation sessions in both contexts, with and without CS+ and CS- presentations. On day 1, the CSs were presented in one of the two contexts, and on day 2 in the other. On days 3 and 4, the rats were fear conditioned in the BOX where CS+ presentations were coupled with foot shocks with similar duration and power as used in previous work (e.g. Giustino et al. 2019, 1 s, 0.6 mA, terminating at end of CS+ presentations). Only CS+ presentations were analyzed.

Data acquisition and processing Brain activity was recorded with a 256-channel digital data acquisition system (KJE-1001, Amplipex, Szeged, Hungary). The signals were acquired with four 64-channel headstages (Amplipex HS2) and sampled wideband at 20 kHz. An inertial measurement unit sampled the 3D angular velocity and linear acceleration of the head at 300 Hz. To determine the instantaneous position of the animal, a red LED mounted on the headstage was imaged by overhead webcams at 30 Hz. Animal behavior was also recorded at 50 Hz by lateral video cameras (acA25000, Basler). Off-line spike sorting was performed using KlustaKwik (K.D. Harris, http://klustakwik.sourceforge.net). The resulting clusters were visually inspected using Klusters[45] to reject noise and to merge units erroneously considered as different units. Neurophysiological and behavioral data were explored using NeuroScope[45]. LFPs were derived from wideband signals by downsampling all channels at 1250 Hz.

Scoring of behavioral and brain states Automatic detection of immobility was performed by thresholding the angular speed calculated from gyroscopic data as described in[46]. LFP data was visualized using Neuroscope[45] and slow-wave sleep (SWS) and freezing were detected as previously described[35].

Histological identification of recording sites At the end of the experiments, recording sites were marked with small electrolytic lesions ($\sim$20 µA for 20 s, one lesion per bundle). After a delay of at least three days to permit glial scarring, rats were deeply anesthetized with a lethal dose of pentobarbital, and intracardially perfused with saline (0.9%) followed by paraformaldehyde (4%). Coronal slices (35 µm) were stained with cresyl-violet and imaged with conventional transmission light microscopy. Recording sites were reconstructed by comparing the images with the stereotaxic atlas of[47]. Data recorded in electrodes bundles whose location could not not be identified were discarded from further analyses.

Statistical analysis All statistical analyses were performed in Matlab (MathWorks, Natick, MA), using the Freely Moving Animal Toolbox (http://fmatoolbox.sourceforge.net) and custom written programs. For descriptive statistics, behavioral data was represented with boxplots where the central bar indicates the median, the bottom and top edges indicate the 25th and 75th percentiles; whiskers extend to the most extreme data points, excluding outliers. Datapoints were considered as outliers if they were greater than $q3 + 2.7\sigma(q3–q1)$ or less than $q1–2.7\sigma(q3–q1)$; where σ is the standard deviation, and q1 and q3 are, respectively, the 25th and 75th percentiles of the sample data.

Analysis of population trajectories over time Principal Component Analysis (PCA) of figure 1D was computed on the spike trains of all hippocampal neurons for each rat. The bins corresponding to shocks and the following 10 seconds were removed in order not to bias population activity with the strong shock responses. For each rat, we measured the distance of projections occurring before and after the first CS+ presentation and the distance of temporally shuffled projections and computed the increase in distance between both distance measures (%).

Assessment of freezing and conditioning responses Firing rate responses to freezing events and CS presentations were assessed by analyzing their peri-event firing rate changes. This was computed by zscoring the raw firing rate and subtracting the average baseline firing rate. Baseline was 2.5 s before freezing onsets for freezing responses and 10 s before CS presentations for CS responses.

In order to assess how CS responses changed with learning, we computed the learning induced change of the responses as the average firing rate change in the 10 seconds following CS presentation (as shown in figure 2F) normalized by subtracting the mean response to the first CS.

Analysis firing rate vs. speed relationship In order to study the relationship between neurons firing rate and animals' motor activity we performed linear regressions. For each neuron we performed a linear regression between speed and the firing rate (z-scored and downsampled in 1 s bins) and computed the coefficient of determination. This was performed individually for each neuron with all time bins of all session types. The distributions of the coefficient of determination in dHPC vs. vHPC were then compared.

Correction for speed-related firing rate changes To correct for speed-related changes in firing rate, for each neuron, we performed a linear regression between firing rate and the angular velocity of the animal on the CS-presentation window. We then removed the linear component of the regression from the firing rate of the neuron according to the animal's speed at that time.

Identification of cell assemblies A standard unsupervised method based on principal and independent component analyses (PCA and ICA) detected the co-activation of simultaneously recorded neurons[48] as we described previously[39,40]. Briefly, spike trains were first binned into 15-ms bins and z-scored to generate a z-scored spike count matrix Z, where $Z_{i,j}$ represents the activity of neuron i during time bin j. The same removal of shock-related bins was performed as in the PCA. Principal components (PCs) were computed by eigendecomposition of the correlation matrix of Z. Principal components associated with eigenvalues exceeding the upper bound of the Marchenko-Pastur distribution were considered significant. We then carried out ICA (using the fastICA algorithm of H. Gävert, J. Hurri, J. Särelä, and A. Hyvärinen, http://research.ics.aalto.fi/ica/fastica) on the projection of Z onto the subspace spanned by significant PCs. Independent component (IC) weights were scaled to unit length, and by convention the arbitrary signs of the weights were set so that the highest absolute weight was positive. Members of cell assemblies were identified using Otsu's method to divide the absolute weights into two groups maximizing inter-class variance, and neurons in the group with greater absolute weights were classified as members. Goodness of separation was quantified using Otsu's effectiveness metric, namely the ratio of the inter-class variance to the total variance. This procedure yielded a set of vectors C_i representing the detected cell assemblies. We verified that members of detected assemblies were more synchronous than non-member neurons (**Supp. Fig. 6B**).

SUPPLEMENTARY FIGURES

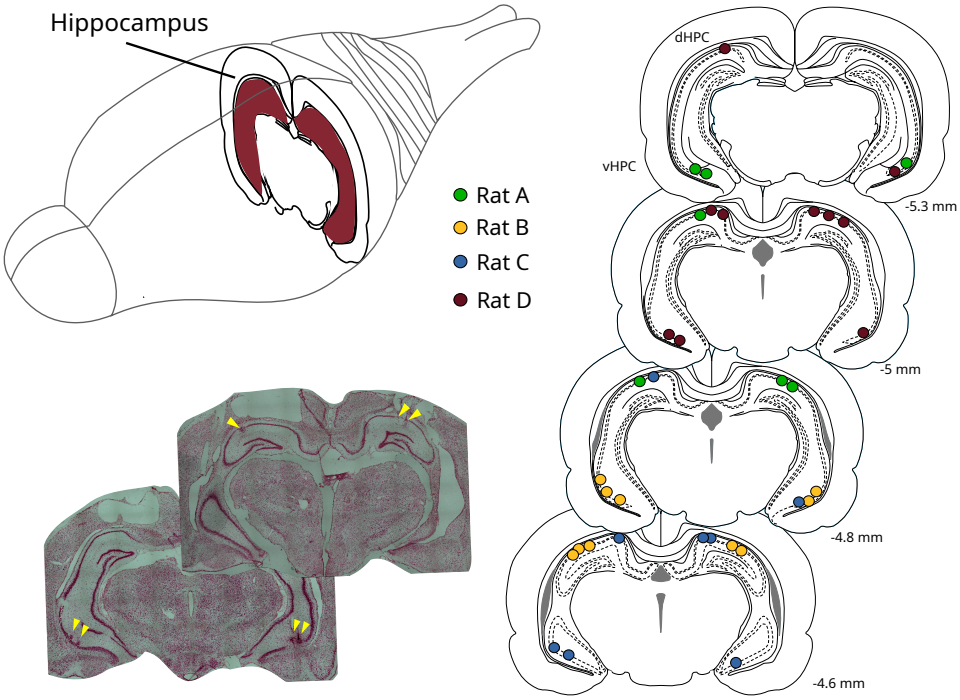

Supplementary Figure 1. **Anatomical reconstruction of the recording sites**.
Sites of electrolytic lesions in the four rats are indicated by the colored circles on the diagrams (right) while the arrows on the images (left) depict some example recording locations in rat B.

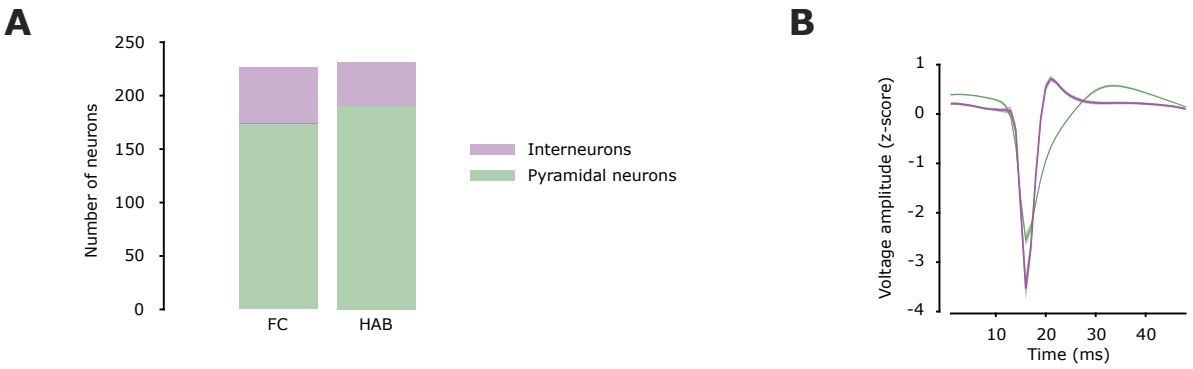

Supplementary Figure 2. Discrimination and quantification of putative interneurons and principal neurons
(**A**) Numbers of interneurons and pyramidal neurons recorded in the FC and HAB sessions
(**B**) Average waveforms for all cells in all rats (same color code as in A, shading represents SEM).

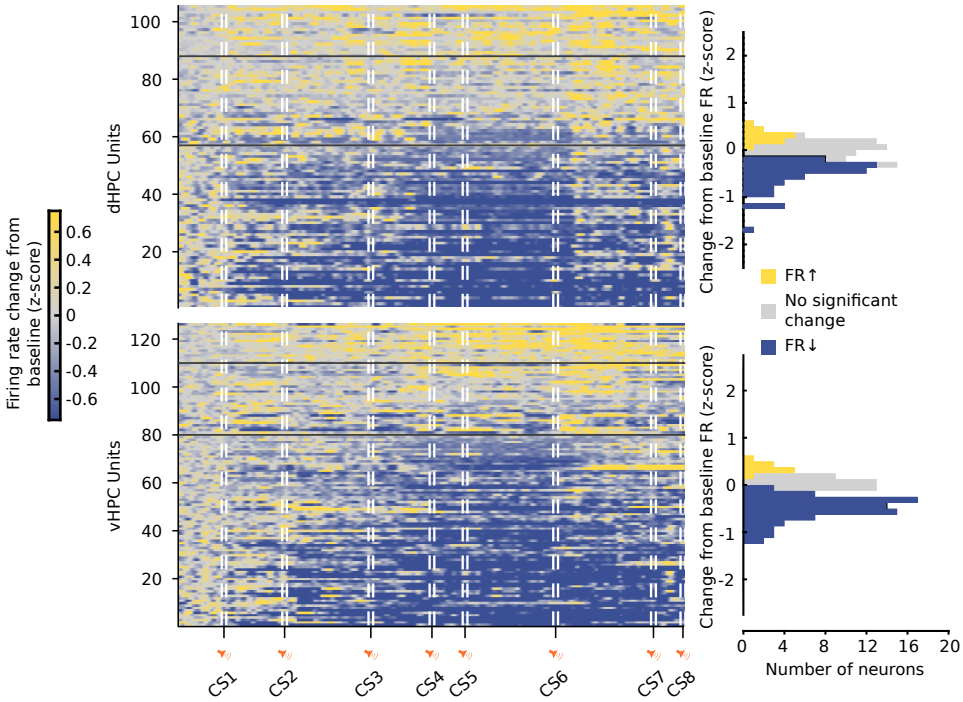

Supplementary Figure 3. Neuronal firing rate changes during habituation sessions.
Color plot of normalized firing rate (z-scored and subtracted relative to baseline) of all neurons during the second HAB session. Baseline: period before the first CS. Horizontal black bars in color rasters separate neurons with significantly ($p < 0.05$) increasing (FR↑), no significant change, and decreasing firing rate (FR↓). Histograms (right) show the distribution of magnitudes of the firing rate changes.

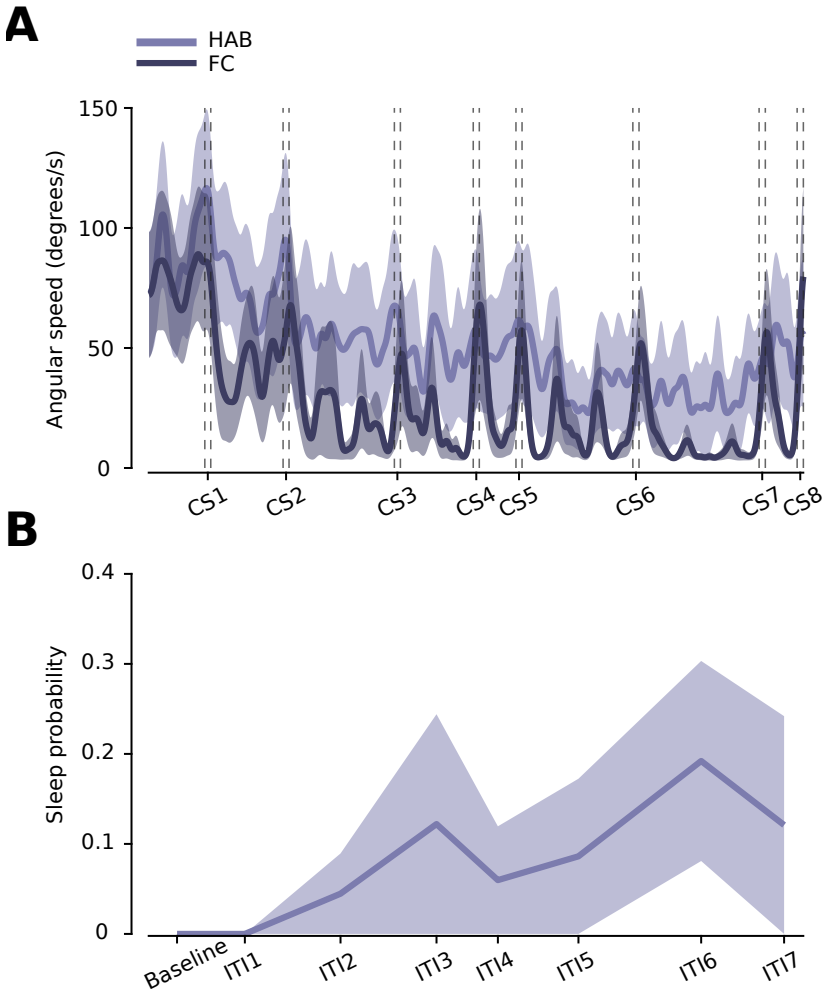

Supplementary Figure 4. Motor activity changes over time.
(**A**) Average speed during HAB (light purple) and FC sessions (dark purple). Shading corresponds to SEM. Peaks at CS presentation correspond to startle responses to the CS and to motor responses to the shock.
(**B**) Average sleep probability during the HAB. No sleep periods were detected during FC.

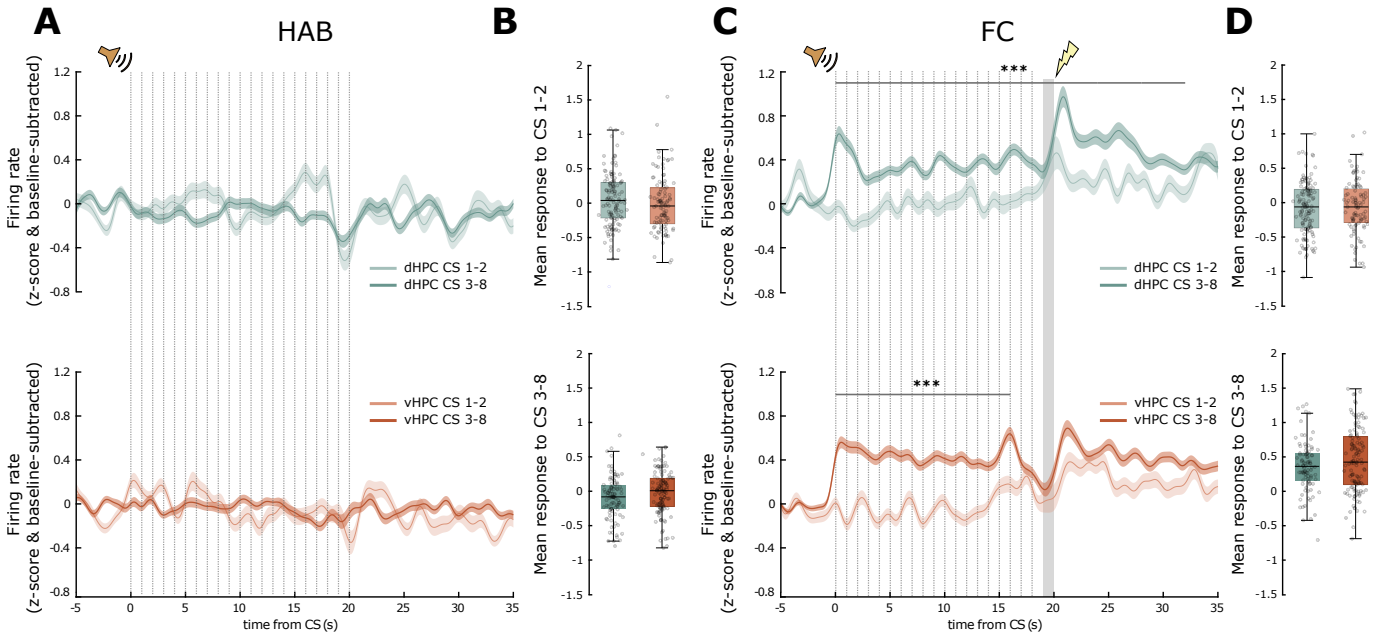

Supplementary Figure 5. Non-speed corrected firing rate responses to CS presentations.
(**A**) Mean firing rate during the second habituation session for CS1 and CS2 (light curves) and CS3 to CS8 (dark curves) for dorsal hippocampal neurons (top) and ventral hippocampal neurons (bottom) (z-scored, baseline-subtracted but not speed-corrected). Same format as Figure 2G.
(**B**) Comparison of the average responses to CS presentations (during the first 10 seconds after the CS) for CS 1-2 (top) and CS 3-8 (bottom) of dorsal (left) and ventral (right) hippocampal neurons. Both comparisons of dHPC vs vHPC are not significantly different. ($p > 0.05$, Wilcoxon signed rank test)
(**C**,**D**). Same as A and B for FC sessions. Again, differences between dHPC and vHPC are not significant

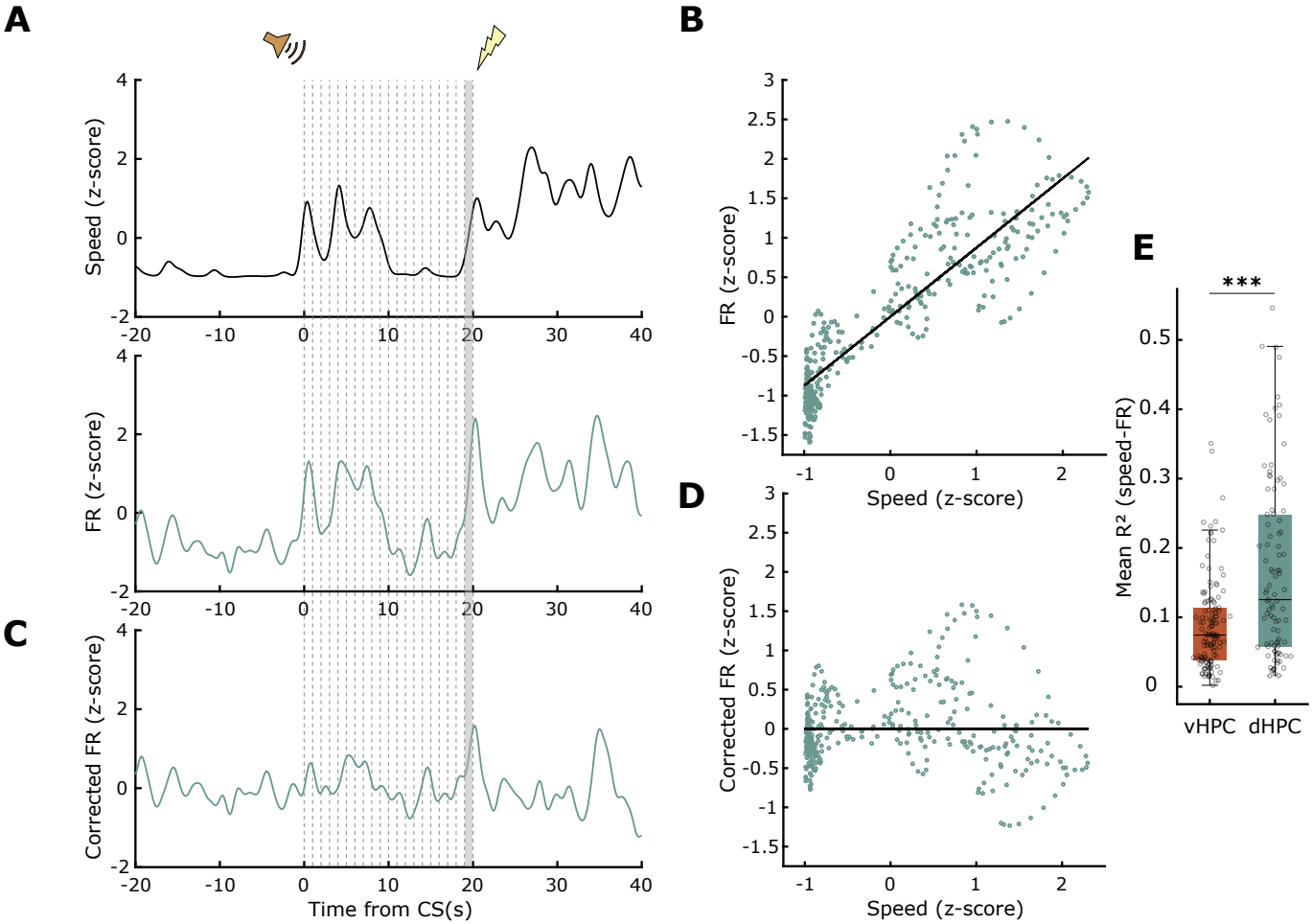

Supplementary Figure 6. Firing rate speed correction.
(**A**) Representative example of the speed (top) and firing rate of a dHPC neuron (bottom) during a 1-minute period, starting 20 seconds before the first CS pip and ending 20 seconds after the last CS pip. Note the speed increase at the first CS presentation, corresponding to a startle response, and the increase in motor activity and firing rate after the shock.
(**B**) Linear regression for angular speed and firing rate for the same period as (A). The concentration of points at z-scored speeds equal to -1 correspond to moments where the animal is immobile.
(**C**) Corrected firing rate for the example in (A) and (B).
(**D**) Linear regression between speed and corrected firing rate.
(**E**) Comparison of coefficients of determination for all dHPC and vHPC neurons computed from data from the same 1-minute periods (averaged over all 8 CSs of FC1 for each neuron).

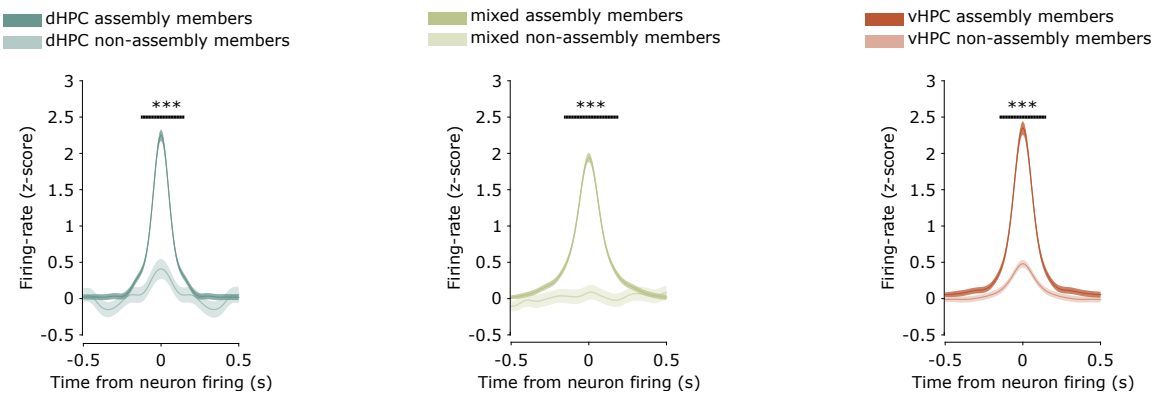

Supplementary Figure 7. Cell assembly synchrony.
Average cross-correlations of the activity of all neuron pairs that were both members of the same assembly vs. randomly selected pairs of neurons that were not members of the same assemblies. Horizontal bars above curves show when average cross-correlations of assembly members were significantly different from non-assembly members ($p < 0.001$, Wilcoxon ranksum test).